

## Rapid Control Prototyping of Five-Level MMC based Induction Motor Drive with different Switching Frequencies

Gopala Venu Madhav<sup>1\*</sup>, T. Anil Kumar<sup>2</sup>, D. Krishna<sup>3</sup>, Ch. Srinivasa Rao<sup>4</sup>,  
Shashank Kumar<sup>5</sup>, Sudipto Poddar<sup>6</sup>

<sup>1,2,3,4</sup> Department of EEE, Anurag University,  
Venkatapur, Ghatkesar, Medchal Dist., Telangana State, India

<sup>5,6</sup> Quarbz Info Systems, Kanpur, India

Correspondence Author : venumadhaveee@cvsr.ac.in

*Received January 25, 2022; Revised February 26, 2022; Accepted March 30, 2022*

### Abstract

In this paper, Rapid Control Prototyping (RCP) of five-level Modular Multilevel Converter (MMC) based Induction Motor (IM) drive performance is observed with different switching frequencies. The Semikron based MMC Stacks with two half-bridge each are tested with the switching logic generated by phase and level shifted based Sinusoidal Pulse Width Modulation (SPWM) technique. The switching logic is generated by the Typhoon Hardware in Loop (HIL) 402. The disadvantages of Multilevel Converter like not so good output quality, less modularity, not scalable and high voltage and current rating demand for the power semiconductor switches can be overcome by using MMC. In this work, the IM drive is fed by MMC and the experimentally the performance is observed. The performance of the Induction Motor in terms of speed is observed with different switching frequencies of 2.5kHz, 5kHz, 7.5kHz, 10kHz, 12.5kHz and the results are tabulated in terms of Total Harmonic Distortion (THD) of input voltage and current to the Induction Motor Drive. The complete model is developed using Typhoon HIL 2021.2 Version Real-Time Simulation Software.

**Keywords:** Rapid Control Prototyping, Modular Multilevel Converter, Sinusoidal Pulse Width Modulation, Induction Motor, Typhoon HIL.

### 1. INTRODUCTION

Power Electronic Converters (PECs) are commonly used in any industrial or power production applications. The reason beyond this is the reduction of the cost of the semiconductor devices(1). For low power applications, generally, single-phase PECs are used, but, for industrial or power production applications, medium or high-power PEC systems are required. Especially, nowadays, the focus is more on renewable energy sources, so there is need to transfer the energy which is available from Solar or Wind to the required load efficiently (2). The role of transferring the energy generated from these renewable energy sources is taken care by the

Power Electronic Inverters, especially, two-level Voltage Source Inverters, Multilevel Inverters, and presently Modular Multilevel Inverters (2, 3). The multilevel converters or MMC can also be used for drive applications such as traction, water pumps, conveyors etc (2, 4).

These High-Power Converters are classified into two types: a) two level converters and b) Multilevel Converters. The Multilevel converters are further classified as: i) integrated type and ii) Multi-Cell type. The integrated type is further classified into four different types, viz., neutral point clamp type, active neutral point clamp type, flying capacitor type and nested neutral point clamp type.

## 2. RELATED WORKS

The Multi-Cell Type Converters are classified into three types: I) Cascaded H-bridge type, II) Cascaded Neutral Point Clamp type and III) Modular Multilevel type. Nowadays, modular approach has been adopted by academia and industries for its benefits like achieving of increased voltage levels and power ratings, maintenance and assembly of power converters is easy, and can be operated during failures, which may not be possible with all the other types mentioned above(5).

Based on the submodule used, the MMC can be classified into two types: a) Half-Bridge MMC and b) Full Bridge or H-Bridge MMC(6). Depending on the number of submodules connected on the upper arm or lower arm of a high-power converter, the voltage level of the MMC can be decided. If 'N' represents the number of submodules of an MMC in each arm then the voltage level of MMC would be  $N+1$ (7). Each submodule is connected with a capacitor which has initial voltage based on the applied DC voltage and it is maintained at its nominal value. The half bridge submodule of an MMC is shown in Figure 1, where C is the capacitance applied across the two Insulated Gate Bipolar Transistors (IGBTs)(8).

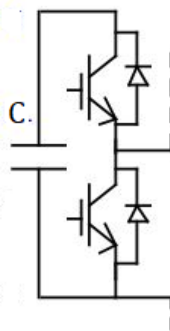


**Figure 1.** Half Bridge Submodule

In this paper, the MMC is applied to a slip ring induction motor which is made to run as squirrel cage induction motor and the machine speed is varied by varying the DC voltage applied to the MMC. MMC considered is the

combination of three stacks of Semikron make two-half bridge type converters.

### 3. ORIGINALITY

Nowadays, testing any medium or high-power applications directly will not be feasible for any organization. So many are adopting to go for Real-Time Simulation of these kinds of applications(9, 10). There are many real-time simulation hardware and softwares which are available to test the complete system proposed. Especially in this category, Hardware-in-the-Loop systems(11, 12) are becoming more and more famous. The authors have presented the work on real-time simulation of MMC for HVDC applications (13). The modelling of MMCs for HVDC application and its real-time simulation is presented in (14). In (15), the authors worked on the real-time simulation of high switching frequency operated power electronic converters, most of the authors in literature have presented the work on FPGA based HIL Real-Time Simulation of power electronic converters. The performance of induction motor drive is verified by simulation and experimental results (13) but the authors didn't focused on the harmonics produced by the back to back modular multilevel converter used in the system. In (14), modular multilevel matrix converter fed doubly fed induction generator is described. The modeling and control of wind energy conversion system has been analyzed in the paper.

The paper (15) presented about the seven-level, five-level, three-level cascaded multilevel inverter fed induction motor drive and analyzed with respect to the total harmonic distortion (THD) of output voltage versus modulation index for three different types of inverters presented and it is verified experimentally. Likewise, in (16), the authors compared the performance of two different levels of MMC fed to induction drive in terms of output voltage THD but not verified experimentally, most of the papers in literature didn't address about the current harmonics. In (17), the authors verified the different Multilevel Converters viz., 3-level H-Bridge Inverter with SPWM, Cascaded H-Bridge 5-level Inverter with SPWM, and Cascaded H-Bridge 7-level Inverter with SPWM fed to BLDC Drive in terms of dominant harmonic frequencies for a switching frequency of 3.05kHz. The paper (18) focused on the arm currents harmonic content in a modular multilevel converter, the analysis says that for the resonant frequencies present due to inductances and capacitances, a given harmonic is only limited and it is verified experimentally but the authors didn't address in terms of an application like motor drive. In this paper, Typhoon Hardware-in-the-Loop (HIL) 402 system is applied and the Typhoon HIL software is used. Rapid Control Prototyping (8, 9) is done for generating the pulses to the half-bridges of the MMCs. The system proposed is being tested for different switching frequencies viz., 2.5kHz, 5 kHz, 7.5 kHz, 10 kHz, and 12.5 kHz and performance of the machine is evaluated in terms of speed control and total harmonic distortion of load currents.

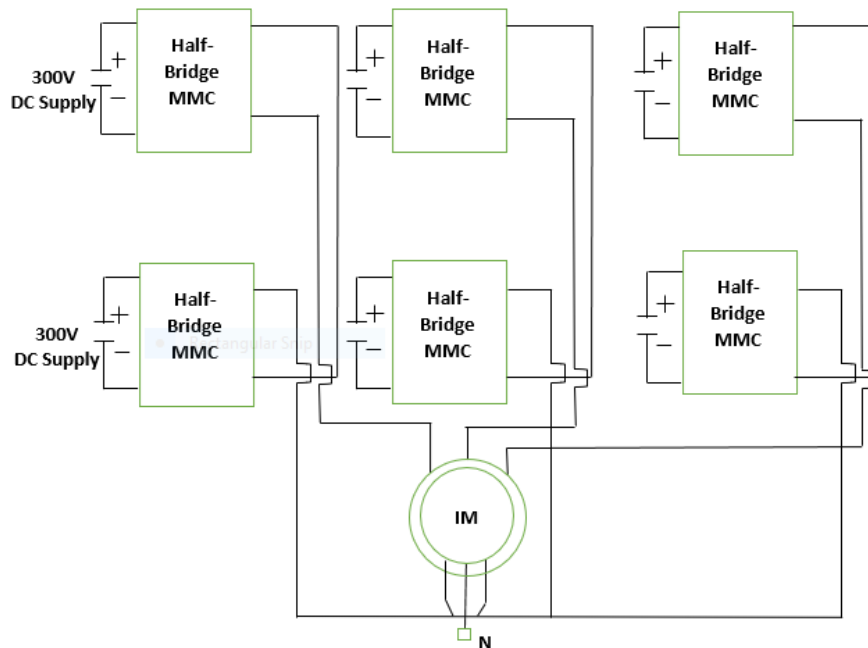


**Figure 2.** Induction Motor (IM) fed with Five Level Modular Multilevel Converter (MMC)

#### 4. SYSTEM DESIGN

The performance analysis of Slip Ring Induction Motor acting as Squirrel Cage Induction Motor for different switching frequencies of converter is analyzed with the implementation of above five level MMC topology. Each MMC stack consists of two half bridge converters, so total three MMC stacks are connected as shown in the Figure 2. Each leg of the converter (the converter considered is acting as inverter) consists of two half bridge converters, these half bridges are supplied (input side) from a DC source of 300V. In real-time experimentation, the DC supply of 300V is taking through an auto transformer (which is supplied with three phase, 415V, 50Hz, AC supply) connected with a rectifier unit. Towards the output side, these half bridges one of the ends are connected in parallel and the other ends are connected to Slip Ring Induction Machine, with one of the ends being connected to the one of the phases of the Stator and the other end connected to the neutral or common node. Thus, making out the three phases of Stator connection from each of the leg of the MMC and the rotor side being short circuited and connecting other ends of converter to a common node or neutral as shown in the **Figure 2** above. Hence, the motor will behave as a Squirrel Cage Induction Machine. In real-time implementation, the above-mentioned circuit diagram is used for the connections of MMC Stacks with the DC supply and the Induction Machine (IM), which is clearly shown in the **Figure 1**.

## 5. PHASE AND LEVEL SHIFT BASED SINUSOIDAL PULSE WIDTH MODULATION (SPWM)

In this section, the modulation technique used for MMC is discussed. SPWM with high frequency switching is used to generate the pulses to the MMC Stack. The switching frequencies considered in this work are 2.5kHz, 5 kHz, 7.5 kHz, 10 kHz, and 12.5 kHz. The performance of the MMC fed induction machine is analyzed for these switching frequencies. As addressed of the various modulation technique's the simplest modulation technique, i.e., SPWM is chosen (19). Further, in the various SPWM techniques, which are classified based on the carrier and modulating signals (11), the phase and level shift based SPWM technique is chosen for generating the pulses to the three stacks of MMCs, which consists of two-bridges each(20, 21). The phase and level shift SPWM technique is also called as Phase Disposition SPWM, in short, PD SPWM. The pulses generated by phase and level shift SPWM technique for 2.5kHz, 5 kHz and 7.5kHz switching frequencies are shown in the Figures 3, 4, and 5 below. In the Figures 3, 4 and 5, all the pulses generated for total six half-bridge MMCs are not shown, for understanding the pulses generated for the top switch of single-phase inverter1 (half-bridge or H-bridge MMC), bottom switch of single-phase inverter1, top and bottom switches of single-phase inverter 3 and top and bottom switches of single-phase inverter6 for 2.5kHz switching frequency are shown, likewise for the switching frequencies of 5kHz and 7.5kHz are also shown in Figures 4 and 5.

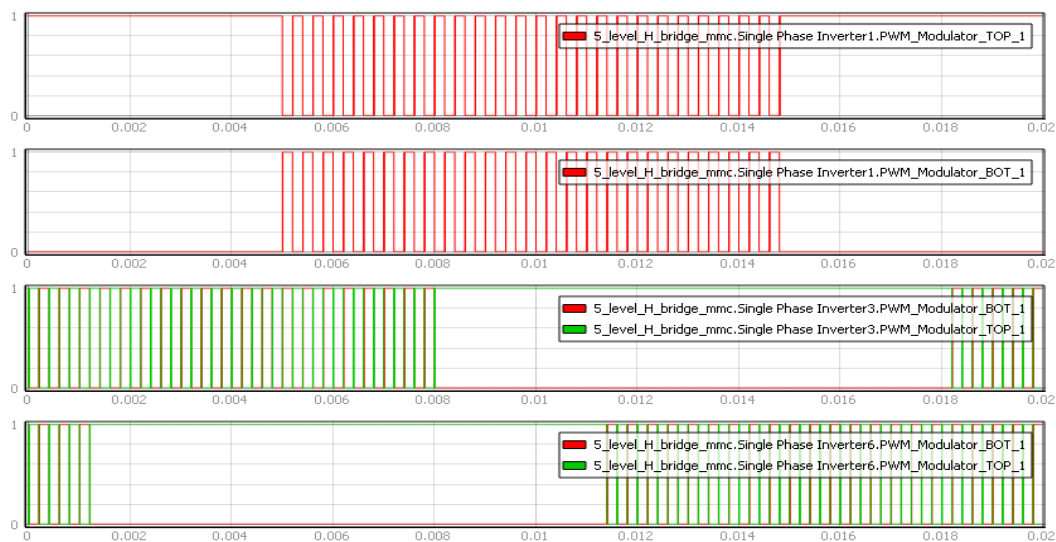


**Figure 3.** Half-Bridge MMC Pulses with Switching Frequency of 2.5kHz.



**Figure 4.** Half-Bridge MMC Pulses with Switching Frequency of 5kHz.



**Figure 5.** Half-Bridge MMC Pulses with Switching Frequency of 7.5kHz.

**6. EXPERIMENT AND ANALYSIS**

The Figure 6. shows the complete experimental setup of five-level Modular Multilevel Converter (MMC) based Wound Rotor Induction Machine (WRIM) using Typhoon HIL 402. Rapid Control Prototyping of the proposed system is carried out and the simulation model of five-level MMC based WRIM, which is acting as Squirrel Cage Induction Motor as the Rotor side ends are short circuited, is developed in Typhoon HIL 2021.2 Version Software. The developed model is simulated in real-time by connecting the laptop with Typhoon HIL software with HIL 402 using USB Cable. The pulses for the IGBTs of MMC are given in real-time through the HIL 402, and the performance of the proposed system can be analyzed with the changes in

parameters. In this project, the performance of the MMC based Induction Motor is analyzed for different values of switching frequencies, and the performance of the motor is analyzed for variation in the input DC voltage to the MMC.

The pulses from the breakout board connected to HIL 402 are given to the MMC by using the level shifters. HIL 402 consists of Xilinx Zynq-7 SoC Processor and 16 Analog Inputs and Outputs and 32 Digital Inputs and Outputs. Apart from that it also consists of ARM processor and Microblaze Processor for computing purpose. For easy connections a breakout board is used which consists of 16 Analog Inputs and Outputs and 32 Digital Inputs and Outputs and 16 Ground pins. In this project, the digital outputs of the pulses including the supply voltage and ground are chosen in Typhoon HIL Software from 1 to 23 alternately and are connected to the level shifters, which are in turn connected to the driver circuit of the MMC.

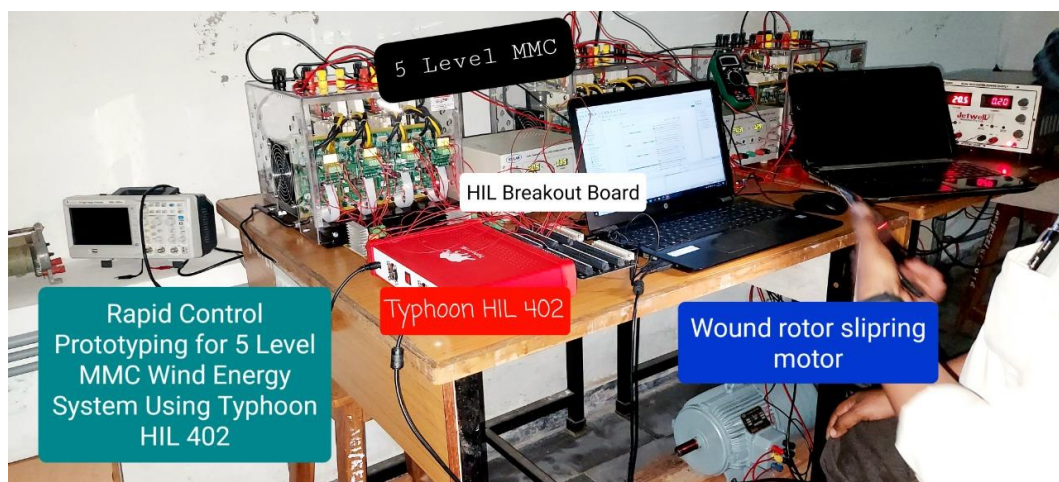


**Figure 6.** Experimental setup of Rapid Control Prototyping of Five-Level MMC based WRIM using Typhoon HIL 402.

The ratings of MMC are: DC link voltage is 300V, output AC voltage is 200V for each bridge, AC current is 10A, switching frequency is 20kHz, fundamental frequency is 50Hz. The ratings of the WRIM are: Rated Power is 3 HP, Rated Voltage is 415V, rated speed is 1440rpm, rated current is 4.7A. The input DC voltage to the MMC is varied by using an auto transformer which is embedded with a rectifier unit. For different switching frequencies of the MMC operation, the performance of the five level MMC fed Induction Motor (IM) is evaluated in terms of speed control by varying the input DC voltage accordingly.

The proposed system is analyzed in Typhoon HIL software by varying the DC input voltage by using slider for different switching frequencies mentioned. The same is verified in real-time RCP of the proposed system and for the both the cases the IM is working efficiently. For RCP of the proposed system when it is experimentally tested with the set up shown in Fig. 6, the machine speed was slowly increasing as the DC input voltage has been

increased, likewise the phase voltage to the IM is also increased slowly, once DC input voltage has reached 175V, the speed of the IM is 626rpm, likewise, for 186V it reached 849rpm, for 196V it reached 1000rpm, for 207V it reached 1127rpm, for 217V it reached 1188rpm and once the DC input voltage reached the maximum value of 300V, the machine speed reached its rated speed of 1440rpm. These values presented are for the switching frequency of 2.5kHz. Figure 7 below shows the Real-Time Simulation results of three-phase load currents ( $I_a$ ,  $I_b$ ,  $I_c$  in A), inverted three-phase AC waveform from MMC ( $V_a$ ,  $V_b$ ,  $V_c$  in V), the line voltage to the IM ( $V_{bc}$ ), the machine speed and torque for switching frequency of 2.5kHz. From the Fig. 7, it can be observed that the switching on and off of the IGBTs leads to distortions in current waveforms, the generation of five-level voltage output to IM, smooth operation of the machine with respect to machine speed. The Fast Fourier Transform (FFT) of the load currents for different switching frequencies is discussed afterwards. Figure 8 shows the expanded waveforms for 2.5kHz switching frequency from 0.4 to 0.5 secs.

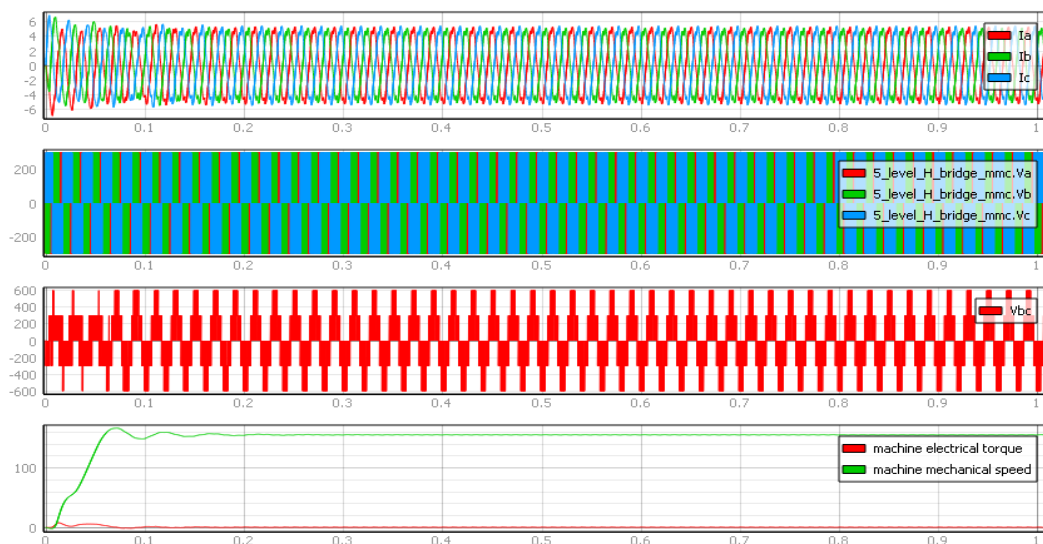


**Figure 7.** Real-Time Simulation Results for Switching Frequency of 2.5kHz (Three-Phase Output Currents of five-level MMC ( $I_a$ ,  $I_b$ ,  $I_c$  in A), Three-Phase Output Voltages of five-level MMC ( $V_a$ ,  $V_b$ ,  $V_c$  in V), Output Line Voltage of five-level MMC ( $V_{bc}$  in V), Machine Speed (rad/s) and Torque (N-m) of IM vs Time (s).

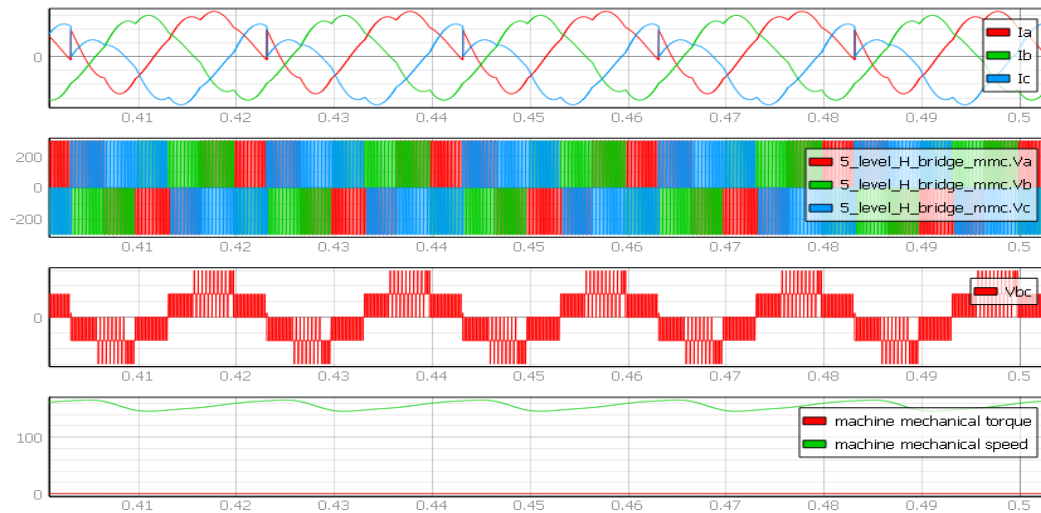


**Figure 8.** Expanded View of Real-Time Simulation Results for Switching Frequency of 2.5kHz (Three-Phase Output Currents of five-level MMC (Ia, Ib, Ic in A), Three-Phase Output Voltages of five-level MMC (Va, Vb, Vc in V), Output Line Voltage of five-level MMC (Vbc in V), Machine Speed (rad/s) and Torque (N-m) of IM vs Time (s).

Similarly, RCP of the proposed system is carried out for switching frequency of 5kHz, the machine speed was slowly increasing as the DC input voltage has been increased, likewise the phase voltage to the IM is also increased slowly, once DC input voltage has reached 198V, the speed of the IM is 1052rpm, likewise, for 233V it reached 1256rpm, for 245V it reached 1290rpm and once the DC input voltage reached the maximum value of 300V, the machine speed reached its rated speed of 1440rpm. These values presented are for the switching frequency of 5kHz. Figure 9 below shows the load currents (Ia, Ib, Ic in A), inverted three-phase AC waveform from MMC (Va, Vb, Vc in V), the line voltage to the IM (Vbc), the machine speed and torque for switching frequency of 5kHz. The results for 5kHz switching frequency are similar to the results of 2.5kHz switching frequency in terms of distortions in output currents, generation of five-level output voltage fed to IM, and smooth operation of IM.

Figure 10 shows the real-time simulation results for switching frequency of 7.5kHz. The results clearly shows that the distortions in the three-phase output currents are increased and after 0.4s the system is stabilizing itself with the phase and level shifted SPWM technique, again the distorted waveform continues. The increase in distortions is evaluated in terms of Total Harmonic Distortion (THD) of output currents, which is explained later. If observed results closely, there is sudden increase in three-phase output voltage (Vc) value and also Vbc value. There are clear oscillations in the machine speed and torque, so experimentally running the IM was not feasible for switching frequencies greater than equal to 7.5kHz.

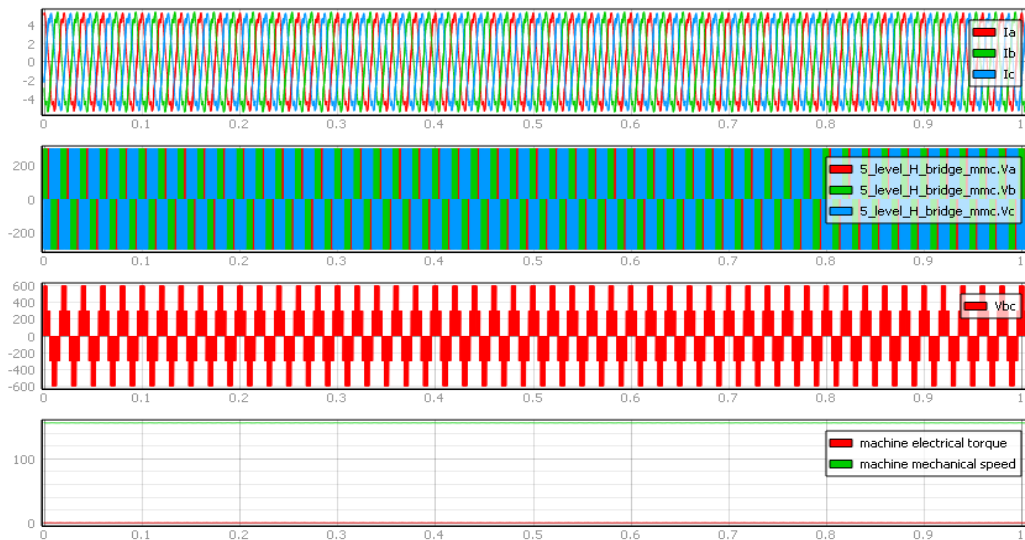


**Figure 9.** Real-Time Simulation Results for Switching Frequency of 5kHz (Three-Phase Output Currents of five-level MMC (Ia, Ib, Ic in A), Three-Phase Output Voltages of five-level MMC (Va, Vb, Vc in V), Output Line Voltage of five-level MMC (Vbc in V), Machine Speed (rad/s) and Torque (N-m) of IM vs Time (s).

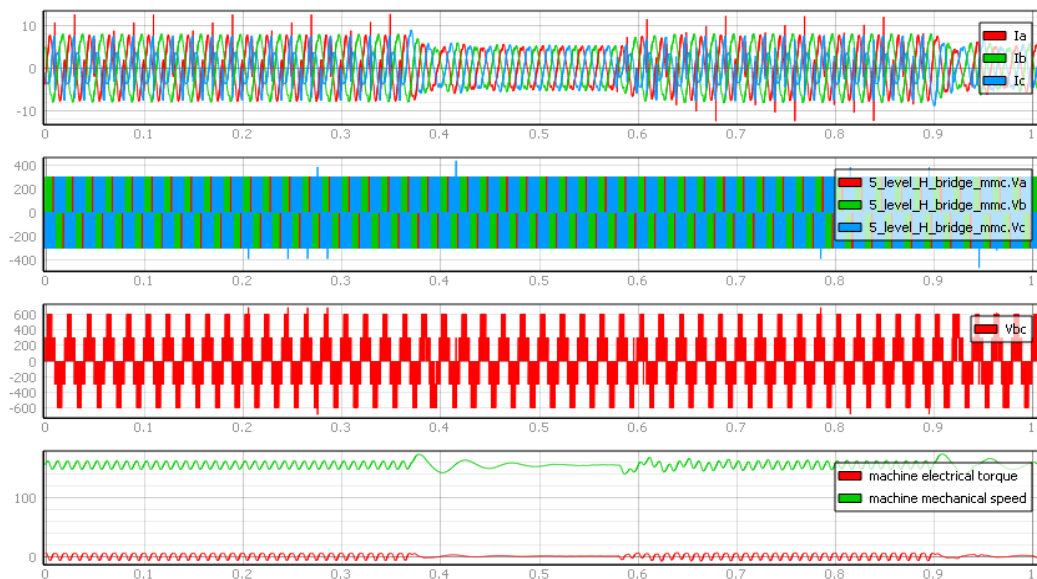


**Figure 10.** Real-Time Simulation Results for Switching Frequency of 7.5kHz (Three-Phase Output Currents of five-level MMC (Ia, Ib, Ic in A), Three-Phase Output Voltages of five-level MMC (Va, Vb, Vc in V), Output Line Voltage of five-level MMC (Vbc in V), Machine Speed (rad/s) and Torque (N-m) of IM vs Time (s).

Figure 11 shows the real-time simulation results for switching frequency of 10kHz. The results clearly shows that the distortions in the three-phase output currents are increased. The increase in distortions is evaluated in terms of Total Harmonic Distortion (THD) of output currents,

which is explained later. There are clear oscillations in the machine speed and torque.

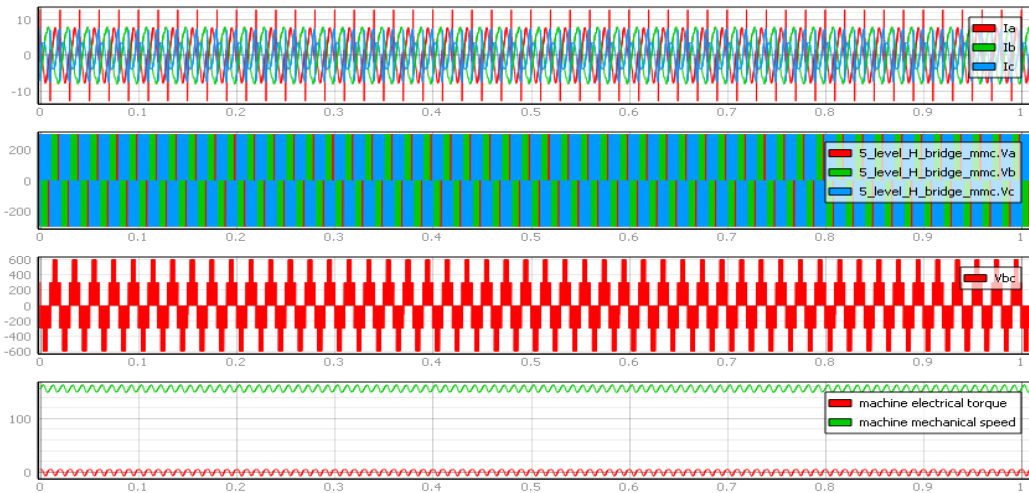


**Figure 11.** Real-Time Simulation Results for Switching Frequency of 10kHz (Three-Phase Output Currents of five-level MMC ( $I_a$ ,  $I_b$ ,  $I_c$  in A), Three-Phase Output Voltages of five-level MMC ( $V_a$ ,  $V_b$ ,  $V_c$  in V), Output Line Voltage of five-level MMC ( $V_{bc}$  in V), Machine Speed (rad/s) and Torque (N-m) of IM vs Time (s))

Figure 12 shows the real-time simulation results for switching frequency of 12.5kHz. The results clearly shows that the distortions in the three-phase output currents are increased. The increase in distortions is evaluated in terms of Total Harmonic Distortion (THD) of output currents, which is explained later. There are clear oscillations in the machine speed and torque.

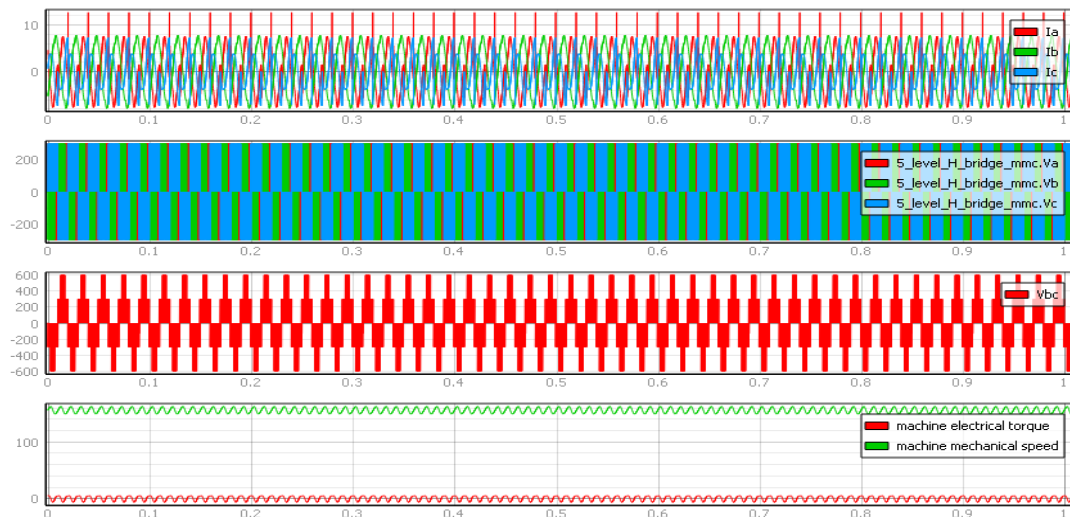


**Figure 12.** Real-Time Simulation Results for Switching Frequency of 12.5kHz (Three-Phase Output Currents of five-level MMC ( $I_a$ ,  $I_b$ ,  $I_c$  in A), Three-Phase Output Voltages of five-level MMC ( $V_a$ ,  $V_b$ ,  $V_c$  in V), Output Line Voltage of five-level MMC ( $V_{bc}$  in V), Machine Speed (rad/s) and Torque (N-m) of IM vs Time (s)).

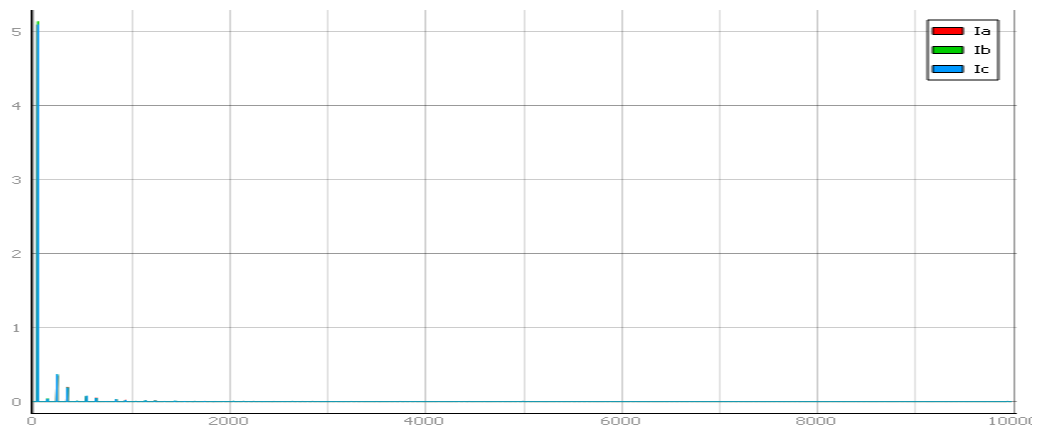
Figure 13a shows that there are lower order harmonics in three-phase output currents for switching frequency of 2.5kHz and there are less magnitude triplen harmonics(odd multiples of third harmonic), and the magnitude of 5th, 7th, 11th, 13th harmonics decreases as the harmonic number increases, which can be observed in the expanded view of FFT of 2.5kHz shown in Fig. 13b. Figure 13c shows the FFT for 5kHz is same as that of 2.5kHz but once the switching frequency is switched to 7.5kHz, shown in Fig. 13d, there is harmonic content and the magnitudes of the 3rd, 5th, 7th etc., harmonics is increased. The FFT for switching frequencies 10kHz and 12.5kHz (shown in Fig.s 13e, 13f respectively) are almost same with little bit variation of the magnitudes of the 3rd, 5th, 7th etc., harmonics compared to 7.5kHz.



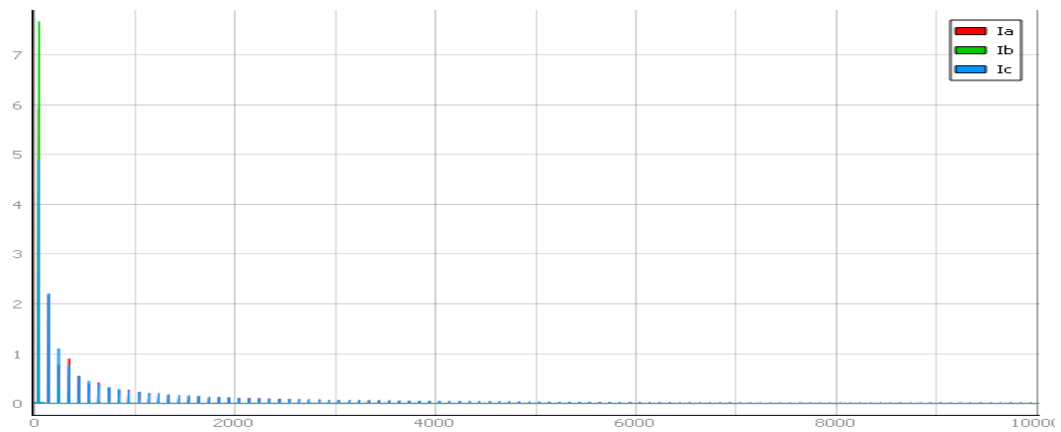
(a)



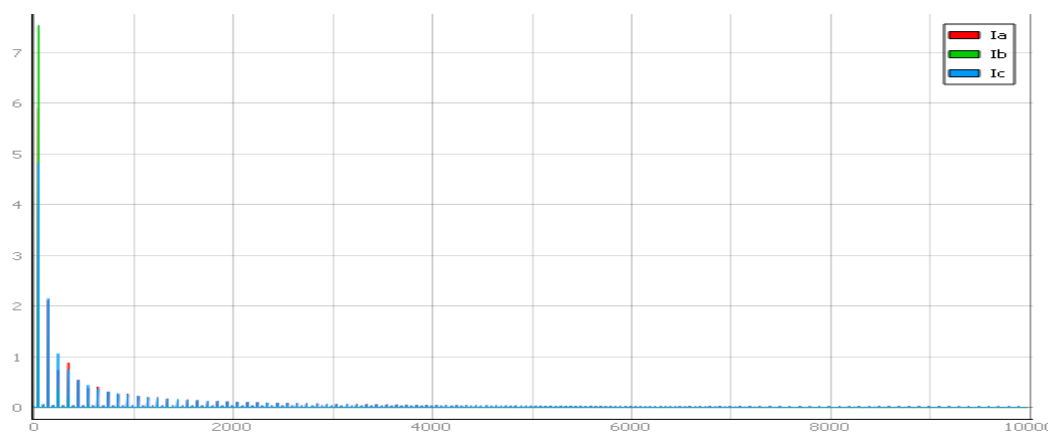
(b)



(c)



(d)



(e)

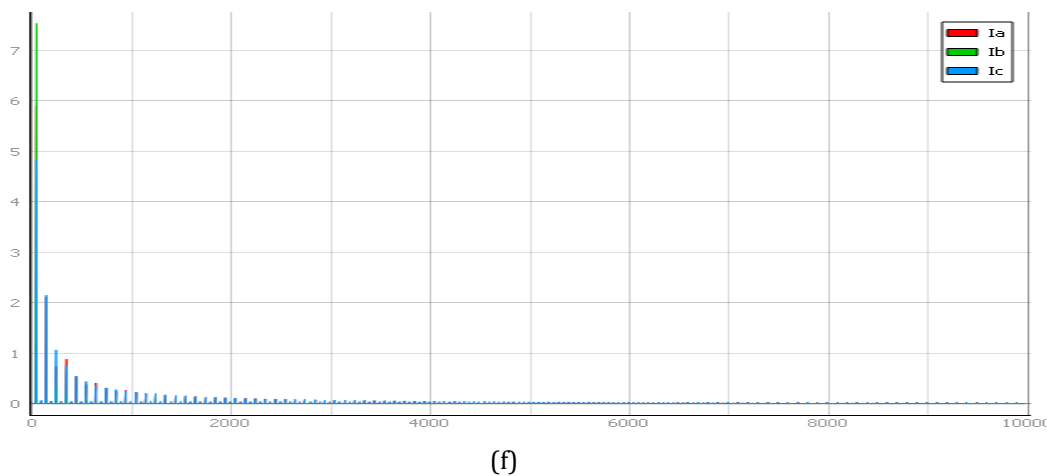
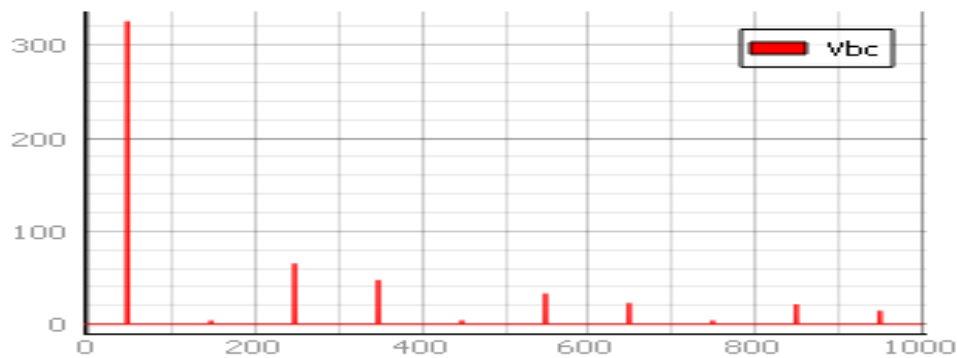
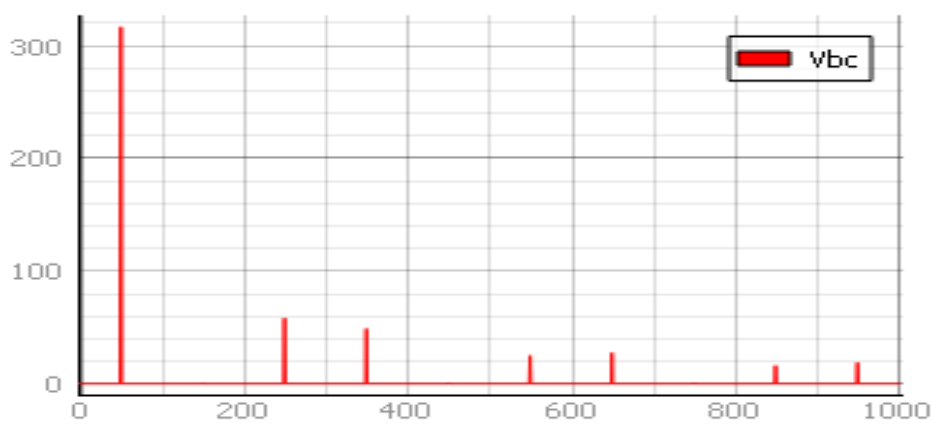


**Figure 13.** Fast Fourier Transform (FFT) of Three-Phase Output Currents for different switching frequencies a) 2.5kHz b) expanded view for 2.5kHz c) 5kHz d) 7.5kHz e) 10kHz f) 12.5kHz

Figure 14a and 14b shows the FFT analysis for line voltage fed to IM, which clearly indicates that there is reduction in magnitude of 5th, 7th, 11th harmonics for 5kHz and 12.5kHz respectively. Further, Figs 14a and 14b, clearly shows that the triplen harmonics are eliminated in Vbc for 12.5kHz switching frequency compared to 5kHz because of the phase and level shift type SPWM modulation technique, that is, it is again proven that the distortion or harmonic content would be reduced in the three phase voltages as the switching frequency increases.



(a)



(b)

**Figure 14.** Fast Fourier Transform (FFT) of Line Voltage  $V_{bc}$  for different switching frequencies a) expanded view for 5kHz b) expanded view for 12.5kHz

**Table 1.** Total Harmonic Distortion (THD) Values of Output Currents (not in terms of percentage) for switching frequencies

Switching Frequency	2.5kHz	5kHz	7.5kHz	10kHz	12.5kHz
<b>THD values of Output Currents (<math>I_a</math>)</b>	0.02	0.02	0.18	0.17	0.17
<b><math>I_b</math></b>	0.08	0.08	0.07	0.05	0.05
<b><math>I_c</math></b>	0.08	0.08	0.48	0.57	0.58

The THD values are same for 2.5kHz, 5kHz and once the circuit operation is verified for 7.5kHz, the THD values varies for  $I_a$  the minimum value is 0.04 and maximum value is 0.18, likewise, for  $I_b$  the minimum value is 0.05 and maximum value is 0.27, for  $I_c$  the minimum value is 0.08 and maximum value is 0.60. The average values of THD for  $I_a$ ,  $I_b$ ,  $I_c$  are 0.18, 0.07, and 0.48. Once switching frequency is increased to 10kHz, 12.5kHz, the THD values of  $I_a$  and  $I_b$  remains same for both the frequencies i.e., 0.17 and 0.05 but there is a slight increase in THD value of load current  $I_c$  from 0.57 to 0.58 as shown in the Table I. Clearly, there is an increase in THD values from 5kHz

to 7.5kHz and 7.5kHz to 10kHz and 12.5kHz. In real-time simulation of the proposed model, the THD value for Vbc for all cases of switching frequencies is almost zero (actual value being near to 0.01, that is, due to still the presence of fifth, seventh harmonic content as shown in Figure 14.

## 7. CONCLUSION

The performance of the MMC fed IM is analyzed both in Real-Time Simulation and by Rapid Control Prototyping, that is, the speed control of IM is achieved for different switching frequencies, viz., 2.5kHz, 5kHz, 7.5kHz, 10kHz, and 12.5kHz. The results shows that the machine speed is comparatively increased as the switching frequency is increased because of more smoother line voltage waveform, the harmonics are increased in load currents with increase in switching frequencies and the triplen harmonics are eliminated, that is, harmonic content is reduced in the line voltages of the IM as the switching frequency is increased.

## Acknowledgments

The authors have greatly acknowledged the support of AICTE, New Delhi for sanctioning the funding under Research Promotion Scheme (RPS) grants with sanction File number 8-205/RIFD/RPS (POLICY-1)/2018-19.

## REFERENCES

- [1] Mohammed H Rashid, **Power Electronics Handbook**, Academic Press (Canada), Ed. 4, 1037-1114, 2017.
- [2] Kola Muralikumar, P Ponnambalam, **Analysis of Cascaded Multilevel Inverter with a Reduced Number of Switches for Reduction of Total Harmonic Distortion**, *IETE Journal of Research*, Vol. 65, No. 5, pp. 1-14, 2020.
- [3] Ronak A Rana, Sujal A Patel, Anand Muthusamy, Chee woo Lee, Hee-Je Kim, **Review of multilevel voltage source inverter topologies and analysis of harmonics distortions in FC-MLI**, *Electronics*, Vol.8, No. 11, pp. 1329-1366, 2019.
- [4] Jun Wang, Xu Han, Hao Ma, Zhihong Bai, **Analysis and injection control of circulating current for modular multilevel converters**, *IEEE Transactions on Industrial Electronics*, Vol. 66, No. 3, pp. 2280-2290, 2018.
- [5] Tian Liang, Venkata Dinavahi, **Real-time device-level simulation of MMC-based MVDC traction power system on MPSoC**, *IEEE Transactions on Transportation Electrification*, Vol. 4, No. 2, pp. 626-641, 2018.
- [6] Mattia Ricco, Marius Gheorghe, Laszlo Mathe, Remus Teodorescu, **System-on-chip implementation of embedded real-time simulator for modular multilevel converters**, *IEEE Energy Conversion Congress and Exposition (ECCE)*, Cincinnati, pp. 1500-1505, 2017.

- [7] Mikhail Mudrov, Anatoliy Zyuzev, Konstantin Nesterov, Stanimir Valtchev, **Hardware-in-the-loop system numerical methods evaluation based on brush DC-motor model**, *International Conference on Optimization of Electrical and Electronic Equipment (OPTIM) & 2017 Intl Aegean Conference on Electrical Machines and Power Electronics (ACEMP)*, Brasov, pp. 428-433, 2017.
- [8] Wei Li, Jean Bélanger, **An equivalent circuit method for modelling and simulation of modular multilevel converters in real-time HIL test bench**, *IEEE Transactions on Power Delivery*, Vol. 31, No. 5, pp. 2401-2409, 2016.
- [9] Potnuru Devendra, Ch Saibabu, **Design and implementation methodology for rapid control prototyping of closed loop speed control for BLDC motor**, *Journal of Electrical Systems and Information Technology*, Vol. 5, No. 1, pp. 99-111, 2018.
- [10] Krisztian Horváth, Marton Kuslits, Szilard Lovas, **Model-based control algorithm development of induction machines by using a well-defined model architecture and rapid control prototyping**, *Electrical Engineering*, Vol. 102, No. 3, pp.1-14, 2020.
- [11] E Himabindu E, Gopichand Naik, **Modular current cell topology of seven and fifteen level csi with reduced count**, *International Journal of Innovative Technology and Exploring Engineering*, Vol. 8, No. 8, pp. 2174-2178, 2019.
- [12] Luc-Andre Gregoire, Kamal Al-Haddad, Girish Nanjundaiah, **Hardware-in-the-Loop (HIL) to reduce the development cost of power electronic converters**, *International Conference on Power Electronics 2010 (ICPE2010)*, New Delhi, pp. 1-6, 2010.
- [13] Mauricio Espinoza, Roberto Cárdenas, Matias Díaz, Andres Mora, Diego Soto, **Modelling and control of the modular multilevel converter in back to back configuration for high power induction machine drives**, *42nd Annual Conference of the IEEE Industrial Electronics Society*, Florence, pp. 5046-5051, 2016.
- [14] Carlos Melendez, Matias Diaz, Felix Rojas, Roberto Cardenas, Mauricio Espinoza, **Control of a double fed induction generator based wind energy conversion system equipped with a modular multilevel matrix converter**, *Fourteenth International Conference on Ecological Vehicles and Renewable Energies (EVER)*, Monte-Carlo, pp. 1-11, 2019.
- [15] Yashobanta Panda, **Analysis of cascaded multilevel inverter induction motor drives**, National Institute of Technology (Rourkela), 2010.
- [16] P Ganesh, N Shanmugavadivu, Kr Santha, **Single-Phase 63-Level Modular Multilevel Inverter fed Induction Motor Drive for Solar PV Applications**, *4th International Conference on Electrical Energy Systems (ICEES)*, Chennai, pp. 596-604, 2018.
- [17] A Purna Chandra Rao, Y P Obulesh, Ch Sai Babu, **Analysis and effect of switching frequency and voltage levels on total harmonic**

- distortion in multilevel inverters fed BLDC drive**, *7th International Conference on Intelligent Systems and Control (ISCO)*, Coimbatore, pp. 65-71, 2013.
- [18] Kalle Ilves, Antonios Antonopoulos, Staffan Norrga, Hans-Peter Nee, **Steady-state analysis of interaction between harmonic components of arm and line quantities of modular multilevel converters**, *IEEE Transactions on Power Electronics*, Vol. 27, No. 1, pp. 57-68, 2011.
- [19] T Kranti Kumar, Gopala Venu Madhav, **Comparative analysis of fifteen level cascaded multi-level converter with different control strategies**, *Materials Today: Proceedings*, Vol. 51, No. 1, pp. 2-11, 2021.
- [20] D Krishna, M Sasikala, V Ganesh, **Mathematical modeling and simulation of UPQC in distributed power systems**, *IEEE International Conference on Electrical, Instrumentation and Communication Engineering (ICEICE)*, Karur, pp. 1-5, 2017.
- [21] E Himabindu, D Krishna, Venu Madhav Gopala, **Performance of Intelligent Controller-Based Bearingless Switched Reluctance Motor**, *Advances in Renewable Energy and Electric Vehicles, Springer (Singapore)*, pp. 355-373, 2022.